

Article

Complex Investigations of a Piecewise-Smooth Remanufacturing Bertrand Duopoly Game

Sameh Askar 

Department of Statistics and Operations Research, College of Science, King Saud University, P.O. Box 2455, Riyadh 11451, Saudi Arabia; saskar@ksu.edu.sa or s.e.a.askar@hotmail.co.uk; Tel.: +966-555-88-3742

Abstract: This paper considers a Bertrand competition between two firms whose decision variables are derived from a quadratic utility function. The first firm produces new products with their own prices while the second firm re-manufactures returned products and sells them in the market at prices that may be less than or equal to the price of the first firm. Dynamically, this competition is constructed on which boundedly rational firms apply a gradient adjustment mechanism to update their prices in each period. According to this mechanism and the nature of the competition, a two-dimensional piecewise smooth discrete dynamic map was constructed in order to study the complex dynamic characteristics of the game. The phase plane of the map was divided into two different regions, separated by border curve. The equilibrium points of the map, in each region on where they are defined, were calculated, and their stability conditions were investigated. Furthermore, we conducted a global analysis to investigate the complex structure of the map, such as closed invariant curves, periodic cycles, and chaotic attractors and their basins, which cause qualitative changes as some parameters are allowed to vary.

Keywords: small piecewise smooth; Bertrand game; stability; bifurcation



Citation: Askar, S. Complex Investigations of a Piecewise-Smooth Remanufacturing Bertrand Duopoly Game. *Mathematics* **2021**, *9*, 2558. <https://doi.org/10.3390/math9202558>

Academic Editor: Vladimir A. Plotnikov

Received: 5 September 2021
Accepted: 5 October 2021
Published: 13 October 2021

Publisher's Note: MDPI stays neutral with regard to jurisdictional claims in published maps and institutional affiliations.



Copyright: © 2021 by the author. Licensee MDPI, Basel, Switzerland. This article is an open access article distributed under the terms and conditions of the Creative Commons Attribution (CC BY) license (<https://creativecommons.org/licenses/by/4.0/>).

1. Introduction

In the economy, there are different kinds of competitions that attract both scientific researchers and economists (who study the complex characteristics of these competitions). Studies show that some of these economic models may be chaotic. Here, we must cite the individual who implemented the first trial of such studies, essentially opening the way for more studies about such models. Augustin Cournot introduced the first mathematical model of a duopoly game [1]. A duopoly game is a special 'case' of the oligopoly game, in which only two firms dominate the market. It is more complex than a monopoly, where only one firm dominates the market. Duopoly games assume that firms sell homogeneous goods in the same market, but with independent prices. Consequently, the optimal decisions of these firms are affected by their opponents. Competition in such games is divided into static or dynamic; in this manuscript, we focus on the dynamic. The Cournot and Bertrand models are popular models that describe dynamic competition [2]. In Cournot models, the two firms produce homogeneous commodities; the decision variables here are the quantities they produce. On the other hand, when the decision variables are prices instead of quantities, the model is known as a Bertrand. The Stackelberg game is also interesting [3,4]—it involves two firms, one of which is more powerful than the other. In such a game, the weaker firm does not take action until the stronger firm takes action. The firms are known as the leader and the follower.

Studying the dynamic features of the above-mentioned models shows whether we can make predictions about these models in the long run. Studying the stability of the equilibrium points of such models occurs after modeling; this requires following certain mechanisms, such as bounded rationality and Puu's approach. The latter is not applied much in the literature because it has some disadvantages when studying the stability of the

equilibrium points [5–7]. The bounded rationality mechanism has been intensively applied in many economic games investigated in the literature. More information about this mechanism and its application exists [8–10]. Studying the stability of the equilibrium reveals that such models open the gate toward discovering other complex dynamic characteristics of systems modeling such a game. Characteristics include the coexistence of different types of bifurcations that make the equilibrium points lose their stability and behave chaotically. There are several studies in the literature [11–15] that have reported that those systems lose their stability due to flip and Neimark–Sacker bifurcations; then routes to chaos coexist.

Remanufacturing in the economy is important and requires more analytical and numerical studies to show its benefits. Remanufacturing is the process of disassembling commodities, which are then repaired and collected, and sent back to the line of production to be sold as new products. The firm, known as a third-party company, handles this part of production. Examples of such companies include Xerox, as well as Mercedes-Benz and Ford for car industries [13]. Studies show that most of the current remanufacturing competitions highlight the decisions taken by all competitors involved in the economy. Only a few studies have focused on the complex dynamic features behind this kind of competition. For example, in [13], a remanufacturing Cournot duopoly game was introduced. It shows that the equilibrium point of the game loses its stability due to the coexistence of two types of bifurcations—period doubling and Neimark–Sacker. Furthermore, in [16], a remanufacturing duopoly game was introduced and its characteristics were investigated. The current paper extends the work introduced in [13]. Here, we study the case of Bertrand adopting the inverse demand functions used in [13]. We assume that the preferences adopted by the consumers follow a quadratic utility function that is concave, by which the inverse demand functions of both firms are derived. However the prices derived from this utility are linear, but the analysis given in this paper is rich in extra dynamic features. Our analysis, either analytic or numeric, differs from those given in [13,16]. In the current paper, we introduce a piecewise smooth Bertrand duopoly game, which is entirely different than smooth Bertrand games in the literature, and gives rise to our motivation. The piecewise Bertrand game is more complicated than classic ones and the bifurcation taking place in this game belongs to border-collision bifurcation. In the literature, several works on tackling piecewise smooth maps were discussed. In [17], a two-dimensional discontinuous piecewise linear map was considered. This map described the dynamics of a discrete-time version of a continuous-time fashion cycle model. The bifurcation discussed in this map belongs to the class of border-collision bifurcation. A three-region footloose-entrepreneur economic geography model was introduced in [18]. The map described this geography model as a piecewise map, defined in three regions. Its local and global dynamics and the corresponding bifurcation were discussed in [18]. In [19], a four-region economic geography model was introduced and analyzed as a piecewise map that was defined in four regions, in which regions are differentiated in size and geographical position. The effects of the constraints were discussed in an adaptive segregation model in [20]. In that study, the model was described by a discrete two-dimensional piecewise smooth dynamic map to investigate the dynamics of the entry and exit of two populations into the model described by such a map. The asymmetric case of the map given in [20] was studied in [21]. In [22], the border collision bifurcations of a piecewise adaptive oligopoly model whose demand function was isoelastic was investigated. Discriminatory individual choices may lead to two groups of people of opposite kinds as a result of segregation. People may be separated for different reasons, such as age, sex, language, income, nationality, skin color, etc. This segregation has led to investigations of such piecewise maps. This piecewise characteristic, which is one of the peculiarities of such models, gives rise to a particular kind of bifurcation due to the change of map definition. This kind of bifurcation is related to closed invariant sets (such as attractors, frontiers, manifolds), having contact with the border region on where the map is defined. Such maps are more general and complicated than the traditional smooth maps and only few studies on those maps have been reported in the literature and its applications to economic models are still undeveloped areas.

In brief, this paper is organized as follows. In Section 2, the piecewise smooth Bertrand map describing the proposed game is formulated. In Section 3, the stability conditions for the equilibrium points in each region where the map is defined are discussed. In Section 4, local and global analyses based on numerical experiments are investigated. Finally, we summarize our obtained results in this paper in the conclusion section.

2. The Model

In an economic market, individuals have their own preferences, which are used to measure their satisfaction about certain goods. Those preferences are translated into decisions of consumers, which are represented according to the demand theory by a utility function. Under a certain budget condition, this utility must be maximized in order to achieve a consumer’s perspective [23]. In this paper, we assume the following utility function,

$$U(q_1, q_2) = q_1 + \theta q_2 - \frac{1}{2}(q_1^2 + 2\theta q_1 q_2 + \theta q_2^2); q_1, q_2 > 0 \tag{1}$$

Which was defined by Singh and Vives [24]. It is easy to see that this function is strictly concave for any values of the decision variables q_1 and q_2 and the fraction parameter θ where $0 < \theta < 1$. The meaning of this fraction is defined later in this section. Now, assume that we have two competing firms. The first firm is called the manufacturer and it produces new goods that are denoted by the variable q_1 , while the second firm receives returned goods and repairs them, and then sells them again in the market. It reproduces the quantity q_2 . Indeed, we restrict the decision variables space to $S = \{(q_1, q_2) : q_1, q_2 > 0\}$. As the first firm is responsible for providing the market with the q_1 at period time t , the second firm should provide the market with returned products at time $t + 1$. Therefore, the consumers will have to differentiate between those products and are willing to pay a fraction θ in order to buy new remanufactured products. Moreover, the second firm’s marginal cost must be less than this fraction θ otherwise it loses the market. So, using a budget constraint $\sum_{i=1}^2 p_i q_i = 1$ with $p_i = \frac{\partial U}{\partial q_i}, i = 1, 2$ and with (1), we obtain the inverse demand functions as follows,

$$\begin{aligned} p_1 &= 1 - q_1 - \theta q_2, \\ p_2 &= \theta(1 - q_1 - q_2) \end{aligned} \tag{2}$$

where $p_i, i = 1, 2$ denotes the price for $q_i, i = 1, 2$. $\theta = 1$ indicates customers’ bias to pay same price for both new and remanufactured goods, which may not be accepted in the economy. $\theta = 0$ means remanufactured goods are not approved by customers. Hence, this variety of preferences gives restrictions of the parameter $\theta \in (0, 1)$. Now, the demand functions of (2) are given by,

$$\begin{aligned} q_1 &= 1 - \frac{1}{1-\theta} p_1 + \frac{1}{1-\theta} p_2, \\ q_2 &= \frac{1}{1-\theta} p_1 + \frac{1}{\theta(1-\theta)} p_2 \end{aligned} \tag{3}$$

Using linear cost functions, $C_i(q_i) = c_i q_i, i = 1, 2$ where $c_i, i = 1, 2$ are the marginal costs. This gives the following profits,

$$\begin{aligned} \pi_1 &= (p_1 - c_1) \left(1 - \frac{1}{1-\theta} p_1 + \frac{1}{1-\theta} p_2 \right), \\ \pi_2 &= (p_2 - c_2) \left(\frac{1}{1-\theta} p_1 + \frac{1}{\theta(1-\theta)} p_2 \right) \end{aligned} \tag{4}$$

Using (4), the marginal profits become:

$$\begin{aligned} \frac{\partial \pi_1}{\partial p_1} &= 1 + \frac{c_1}{1-\theta} - \frac{2}{1-\theta} p_1 + \frac{1}{1-\theta} p_2, \\ \frac{\partial \pi_2}{\partial p_2} &= \frac{c_2}{\theta(1-\theta)} - \frac{2}{\theta(1-\theta)} p_2 + \frac{1}{1-\theta} p_1 \end{aligned} \tag{5}$$

By setting $\frac{\partial \pi_i}{\partial p_i} = 0, i = 1, 2$ the equilibrium point $E = (\bar{p}_1, \bar{p}_2)$ for the firms is unique and takes the following form:

$$\begin{aligned} \bar{p}_1 &= \frac{2(1+c_1-\theta)+c_2}{4-\theta}, \\ \bar{p}_2 &= \frac{\theta(1+c_1-\theta)+2c_2}{4-\theta} \end{aligned} \tag{6}$$

It depends on the parameters c_1, c_2 and θ . Let us first show the influence of the parameter θ on the equilibrium point. It is easy to get,

$$\begin{aligned} \frac{\partial \bar{p}_1}{\partial \theta} &= \frac{2c_1+c_2-6}{(4-\theta)^2}, \\ \frac{\partial \bar{p}_2}{\partial \theta} &= \frac{\theta^2-8\theta+4+2(2c_1+c_2)}{(4-\theta)^2} \end{aligned} \tag{7}$$

This means that $\frac{\partial \bar{p}_1}{\partial \theta} < 0$ under the condition $2c_1 + c_2 < 6$ and $\frac{\partial \bar{p}_2}{\partial \theta} > 0$ is always satisfied for $\theta^2 - 8\theta + 4 + 2(2c_1 + c_2) > 0$ and $0 < \theta < 1$. This means that by increasing the parameter θ , the price of the remanufactured goods will be high and the price of the new goods will decrease. However, in the economy, consumers prefer to buy new goods instead of buying remanufactured goods; therefore, it may be preferable to keep the fraction θ low for both firms. Now, we assume a repeated discrete dynamic games between the two firms according to their prices (the so-called Bertrand game). To do that, we recall the bounded rationality mechanism [25–27]. This mechanism depends on the change occurring in the marginal profit, $\Phi_i(p_1, p_2) = \frac{\partial \pi_i}{\partial p_i}, i = 1, 2$, whether it is increased or decreased. It is expressed as follows,

$$p_i(t + 1) = p_i(t) + k_i(p_i)\Phi_i(p_1, p_2), i = 1, 2 \tag{8}$$

where, $k_i(p_i)$ refers to an adjustment parameter. This parameter is important in such games and has influences on the stability of the equilibrium point of the game. Using (5) and (8) and assuming that $\alpha_i(q_i) = k_i p_i, i = 1, 2$ the following discrete dynamic system is obtained.

$$\begin{aligned} p_{1,t+1} &= p_{1,t} + k_1 p_{1,t} \left(1 + \frac{c_1}{1-\theta} - \frac{2}{1-\theta} p_{1,t} + \frac{1}{1-\theta} p_{2,t} \right), \\ p_{2,t+1} &= p_{2,t} + k_2 p_{2,t} \left(\frac{c_2}{\theta(1-\theta)} - \frac{2}{\theta(1-\theta)} p_{2,t} + \frac{1}{1-\theta} p_{1,t} \right) \end{aligned} \tag{9}$$

where $k_i, i = 1, 2$ is positive constant. Here, we should mention that the price of the second firm at time $t + 1$ should be less than or equal those of the first firm at time t , i.e., $p_2(t + 1) \leq p_1(t)$. Therefore, the system defined by (9) should be modified to: $p_2(t + 1) = \min\{\Omega(t), p_1(t)\}$ where $\Omega = p_2(t) + k_2 p_2 \left(\frac{c_2}{\theta(1-\theta)} - \frac{2}{\theta(1-\theta)} p_2 + \frac{1}{1-\theta} p_1 \right)$ then the system (9) is rewritten to,

$$\begin{aligned} p_{1,t+1} &= p_{1,t} + k_1 p_{1,t} \left(1 + \frac{c_1}{1-\theta} - \frac{2}{1-\theta} p_{1,t} + \frac{1}{1-\theta} p_{2,t} \right), \\ p_{2,t+1} &= \min\{\Omega(t), p_1(t)\} \end{aligned} \tag{10}$$

Therefore, the map defined in (10) is considered as a piecewise map. In order to study the stability of this map, one should consider the second equation in the above map. It is governed by the function Ω . This function is responsible for converting the map (9) to a piecewise one. This means that if $(p_1, p_2) \in \Omega$ and $\Omega < p_1$ then we have only one part from the map (10) to be applied, otherwise if $\Omega > p_1$ we have the other part of the map to be used. Here comes the case when $\Omega = p_1$, which is called the border curve, in which the map (10) is continuous but not differentiable. This border curve divides the phase plane into different regions where the map is defined by different expressions. It has the following form,

$$p_1 = \frac{p_2 \left[1 + \frac{k_2}{\theta(1-\theta)} (c_2 - 2p_2) \right]}{1 - \frac{k_2}{1-\theta} p_2} := g(p_2) \tag{11}$$

that makes the map (10) becomes,

$$\begin{aligned}
 p_{1,t+1} &= p_{1,t} + k_1 p_{1,t} \left(1 + \frac{c_1}{1-\theta} - \frac{2}{1-\theta} p_{1,t} + \frac{1}{1-\theta} p_{2,t} \right), \\
 p_{2,t+1} &= \begin{cases} p_{2,t} + k_2 p_{2,t} \left(\frac{c_2}{\theta(1-\theta)} - \frac{2}{\theta(1-\theta)} p_{2,t} + \frac{1}{1-\theta} p_{1,t} \right) & \text{if } p_{1,t} \geq g(p_2) \\ p_{1,t} & \text{if } p_{1,t} \leq g(p_2) \end{cases} \quad (12)
 \end{aligned}$$

or it is equivalent to,

$$\begin{aligned}
 (p_{1,t+1}, p_{2,t+1}) &= \begin{cases} p_{1,t} + k_1 p_{1,t} \left(1 + \frac{c_1}{1-\theta} - \frac{2}{1-\theta} p_{1,t} + \frac{1}{1-\theta} p_{2,t} \right), \\ p_{2,t} + k_2 p_{2,t} \left(\frac{c_2}{\theta(1-\theta)} - \frac{2}{\theta(1-\theta)} p_{2,t} + \frac{1}{1-\theta} p_{1,t} \right) & \text{if } p_{1,t} \geq g(p_2) \text{ (region 1)} \\ p_{1,t} + k_1 p_{1,t} \left(1 + \frac{c_1}{1-\theta} - \frac{2}{1-\theta} p_{1,t} + \frac{1}{1-\theta} p_{2,t} \right), \\ p_{1,t} & \text{if } p_{1,t} \leq g(p_2) \text{ (region 2)} \end{cases} \quad (13)
 \end{aligned}$$

It is important to note that the stability of the above map should be studied according to the border curve. This means that the map may have fixed points that are located in different regions of the phase plane. The destabilization of those fixed points means that their dynamics are usually never related to one region and, hence, the dynamic of the map must be studied as a piecewise map.

3. The Stability

It is clear that the map (13) is defined in two different regions, so there may be different fixed points in each region. We denote the fixed points in these regions by E_{r1} and E_{r2} where $E_{r1} = \left(\frac{2(1+c_1-\theta)+c_2}{4-\theta}, \frac{\theta(1+c_1-\theta)+2c_2}{4-\theta} \right)$ and $E_{r2} = (1 + c_1 - \theta, 1 + c_1 - \theta)$. The Jacobians at those points are,

$$\begin{aligned}
 J_{r1} &= \begin{bmatrix} 1 - \frac{2k_1(1+c_1)[2(c_2+\theta)-\theta^2]}{4(1+c_1)(1+c_2)-\theta^2} & \frac{-\theta k_1[2(c_2+\theta)-\theta^2]}{4(1+c_1)(1+c_2)-\theta^2} \\ \frac{-\theta^2 k_2(1+2c_1)}{4(1+c_1)(1+c_2)-\theta^2} & 1 - \frac{2\theta k_2(1+2c_1)(c_2+\theta)}{4(1+c_1)(1+c_2)-\theta^2} \end{bmatrix}, \\
 J_{r2} &= \begin{bmatrix} 1 - \frac{2k_1(1+c_1)}{\theta+2(1+c_1)} & \frac{-\theta k_1}{\theta+2(1+c_1)} \\ 1 & 0 \end{bmatrix} \quad (14)
 \end{aligned}$$

Studying the stability of those fixed points depends on the eigenvalues that are calculated by $\lambda_{1,2} = \frac{1}{2}(\tau \pm \sqrt{\tau^2 - 4\delta})$. Where τ and δ refer to the trace and determinant respectively. They are depending on the region on where the fixed points lie in. There may be τ_{r1} or τ_{r2} if the fixed points lie in region 1 or region 2. The same observation is for δ (δ_{r1} or δ_{r2}). They are given by,

$$\begin{aligned}
 \tau_{r1} &= 2 \left[1 - k_1 \left(\frac{c_2+2(1+c_1-\theta)}{(4-\theta)(1-\theta)} \right) - \frac{k_2}{\theta} \left(\frac{2c_2+\theta(1+c_1-\theta)}{(4-\theta)(1-\theta)} \right) \right], \\
 \tau_{r2} &= 1 - \frac{2(1+c_1-\theta)}{1-\theta} k_1, \\
 \delta_{r1} &= 1 - 2k_1 \left(\frac{c_2+2(1+c_1-\theta)}{(4-\theta)(1-\theta)} \right) - \frac{2k_2}{\theta} \left(\frac{2c_2+\theta(1+c_1-\theta)}{(4-\theta)(1-\theta)} \right) - k_1 k_2 \left(1 - \frac{4}{\theta^2} \right) \left(\frac{c_2+2(1+c_1-\theta)}{(4-\theta)(1-\theta)} \right) \left(\frac{2c_2+\theta(1+c_1-\theta)}{(4-\theta)(1-\theta)} \right), \\
 \delta_{r2} &= -\frac{(1+c_1-\theta)}{1-\theta} k_1 \quad (15)
 \end{aligned}$$

The eigenvalues in both regions are,

$$\begin{aligned}
 \lambda_{1r1,2r1} &= 1 - k_1 \left(\frac{c_2+2(1+c_1-\theta)}{(4-\theta)(1-\theta)} \right) - \frac{k_2}{\theta} \left(\frac{2c_2+\theta(1+c_1-\theta)}{(4-\theta)(1-\theta)} \right) \pm \\
 &\quad \pm \frac{1}{\theta} \sqrt{\theta^2 k_1^2 \left(\frac{c_2+2(1+c_1-\theta)}{(4-\theta)(1-\theta)} \right)^2 - \theta(1-\theta) k_1 k_2 \left(\frac{c_2+2(1+c_1-\theta)}{(4-\theta)(1-\theta)} \right) \left(\frac{2c_2+\theta(1+c_1-\theta)}{(4-\theta)(1-\theta)} \right) + k_2^2 \left(\frac{2c_2+\theta(1+c_1-\theta)}{(4-\theta)(1-\theta)} \right)^2}, \\
 \lambda_{1r2,2r2} &= \frac{1}{2} - k_1 \left(\frac{1+c_1-\theta}{1-\theta} \right) \pm \frac{1}{2} \sqrt{1 + 4k_1^2 \left(\frac{1+c_1-\theta}{1-\theta} \right)^2} \quad (16)
 \end{aligned}$$

Or it can be rewritten in the form,

$$\begin{aligned} \lambda_{1r1,2r1} &= \frac{1}{2} \left(\tau_{r1} \pm \sqrt{\tau_{r1}^2 - 4\delta_{r1}} \right) \\ \lambda_{1r2,2r2} &= \frac{1}{2} \left(\tau_{r2} \pm \sqrt{\tau_{r2}^2 - 4\delta_{r2}} \right) \end{aligned}$$

It should be noted that the map (13) is continuous and differentiable in both regions separately. However, on the border curve $\Omega = p_1$, the map is continuous, but not differentiable. Furthermore, there may be no fixed point in one region of the phase plane. This means that the fixed point E_{r1} (or E_{r2}) may turn out to be in region 2 (or region 1). This also means that the character of a virtual fixed point exists. In addition, the stability of those fixed points will be governed by the following triangles,

$$\begin{aligned} S_{r1} &= \{(\tau_{r1}, \delta_{r1}) : 1 + \tau_{r1} + \delta_{r1} > 0, 1 - \tau_{r1} + \delta_{r1} > 0, 1 - \delta_{r1} > 0\} \\ S_{r2} &= \{(\tau_{r2}, \delta_{r2}) : 1 + \tau_{r2} + \delta_{r2} > 0, 1 - \tau_{r2} + \delta_{r2} > 0, 1 - \delta_{r2} > 0\} \end{aligned} \tag{17}$$

where,

$$\begin{aligned} 1 + \tau_{r1} + \delta_{r1} &= \frac{[c_2+2(1+c_1-\theta)][2c_2+\theta(1+c_1-\theta)]}{\theta(4-\theta)(1-\theta)^2} k_1 k_2, \\ 1 - \tau_{r1} + \delta_{r1} &= 4 - 4 \left(\frac{c_2+2(1+c_1-\theta)}{(4-\theta)(1-\theta)} \right) k_1 - \frac{4}{\theta} \left(\frac{2c_2+\theta(1+c_1-\theta)}{(4-\theta)(1-\theta)} \right) k_2 - \left(1 - \frac{4}{\theta} \right) \left(\frac{c_2+2(1+c_1-\theta)}{(4-\theta)(1-\theta)} \right) \left(\frac{2c_2+\theta(1+c_1-\theta)}{(4-\theta)(1-\theta)} \right) k_1 k_2, \\ 1 - \delta_{r1} &= 2k_1 \left(\frac{c_2+2(1+c_1-\theta)}{(4-\theta)(1-\theta)} \right) + \frac{4}{\theta} \left(\frac{2c_2+\theta(1+c_1-\theta)}{(4-\theta)(1-\theta)} \right) + \left(1 - \frac{8}{\theta^2} \right) \left(\frac{c_2+2(1+c_1-\theta)}{(4-\theta)(1-\theta)} \right) \left(\frac{2c_2+\theta(1+c_1-\theta)}{(4-\theta)(1-\theta)} \right) k_1 k_2, \\ 1 + \tau_{r2} + \delta_{r2} &= \frac{(1+c_1-\theta)}{1-\theta} k_1, \\ 1 - \tau_{r2} + \delta_{r2} &= 2 - \frac{3(1+c_1-\theta)}{1-\theta} k_1, \\ 1 - \delta_{r2} &= -1 + \frac{(1+c_1-\theta)}{1-\theta} k_1 \end{aligned} \tag{18}$$

Now, the next section carries out some numerical simulation in order to investigate the routes and the types of bifurcation by which the fixed points of the above system lose their stability.

4. Numerical Simulation

By looking at the map (13) one can see that it contains five important parameters, k_1, k_2, c_1, c_2 and θ . We start our numerical analysis by investigating the influences of k_1 and k_2 on the stability of the map. Figure 1a,b present 2D-bifurcation diagrams in the (k_1, k_2) -plane at two different sets of parameters' values. These sets are $(\theta, c_1, c_2) = (0.9721801, 0.41, 0.45)$ and $(\theta, c_1, c_2) = (0.74, 0.4, 0.8316)$ for the same datum $(p_{0,1}, p_{0,2}) = (0.12, 0.11)$. Figure 1a shows different colored regions on where different periodic cycles, chaotic attractors, and closed invariant curves coexist due to both Neimark–Sacker and flip bifurcation. Figure 1b presents closed invariant sets due to Neimark–Sacker bifurcation followed by flip bifurcation. Therefore, we study, in the next section, the global influence of the parameters k_1 and k_2 separately in the dynamic of map (13). Now, we study the local impact of these parameters by assuming $(\theta, c_1, c_2, k_2) = (0.9721801, 0.41, 0.45, 0.006)$. Figure 1c presents a situation of stable equilibrium point for any value of the parameter k_1 until this parameter reaches the value 0.061 on where there are two routes to two different types of bifurcations, Neimark–Sacker comes first then followed by flip bifurcation. The same observation is presented in Figure 1d for the variable q_2 . At the parameters set $(\theta, c_1, c_2, k_1) = (0.9721801, 0.41, 0.45, 0.006)$, Figure 1e,f show the bifurcation diagrams for the map's variables when varying the parameter k_2 . Another mixed scenario arises when we assume the following set of parameter values, $(\theta, c_1, c_2) = (0.74, 0.4, 0.8316)$. At this set, the equilibrium point becomes stable when varying either k_1 or k_2 until closed invariant curves are born because of Neimark–Sacker bifurcation. Afterward, higher periodic cycles and chaotic attractors coexist due to flip bifurcation, as shown in Figure 2a,b. This discussion shows that the speeds of the adjustment parameters k_1 and k_2 have a great impact on the map's equilibrium points. There is more evidence by which we confirm that the map enters chaotic regions. The evidence is confirmed by plotting the largest Lyapunov exponent (LLE). It is known that when LLE takes positive values, it means that the map's

dynamic behavior enters chaotic regions and, hence, closed invariant curves or higher period cycles, and then routes to chaos coexist. We show in Figure 2c,d the corresponding LLE for the two cases plotted in Figure 2a,b with respect to the parameters k_1 and k_2 .

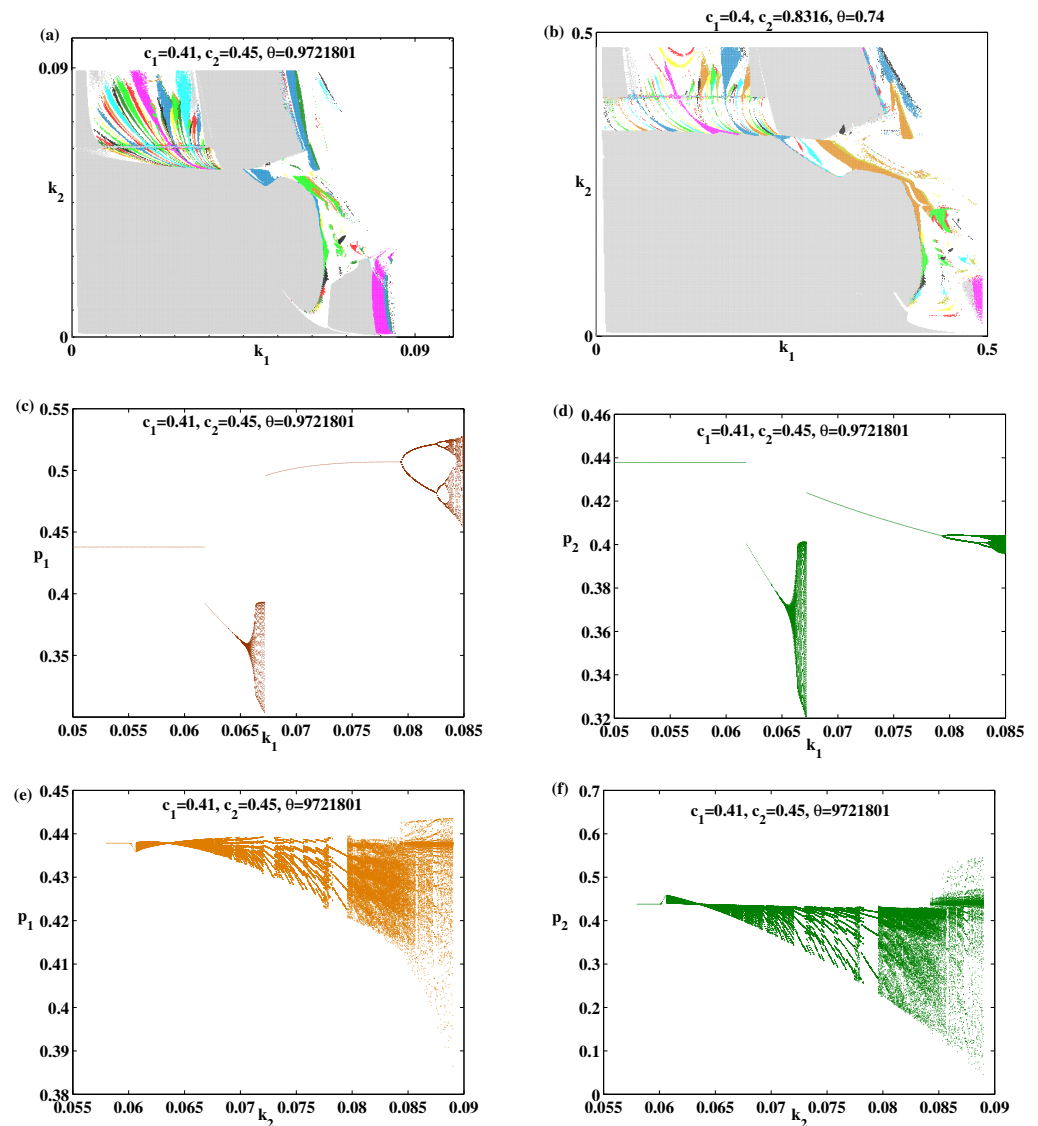


Figure 1. (a,b) 2D bifurcation diagram of the system in the (k_1, k_2) parameter plane. The light gray color refers to the stability region of the fixed point. Other colors are for different types of period cycles. The white color refers to the non-convergent points. (c,d) Bifurcation diagrams with respect to p_1 and p_2 on varying k_1 at: $c_1 = 0.41, c_2 = 0.45, \theta = 0.9721801$ and $k_2 = 0.006$. (e,f) Bifurcation diagrams with respect to p_1 and p_2 on varying k_2 at: $c_1 = 0.41, c_2 = 0.45, \theta = 0.9721801$ and $k_1 = 0.006$.

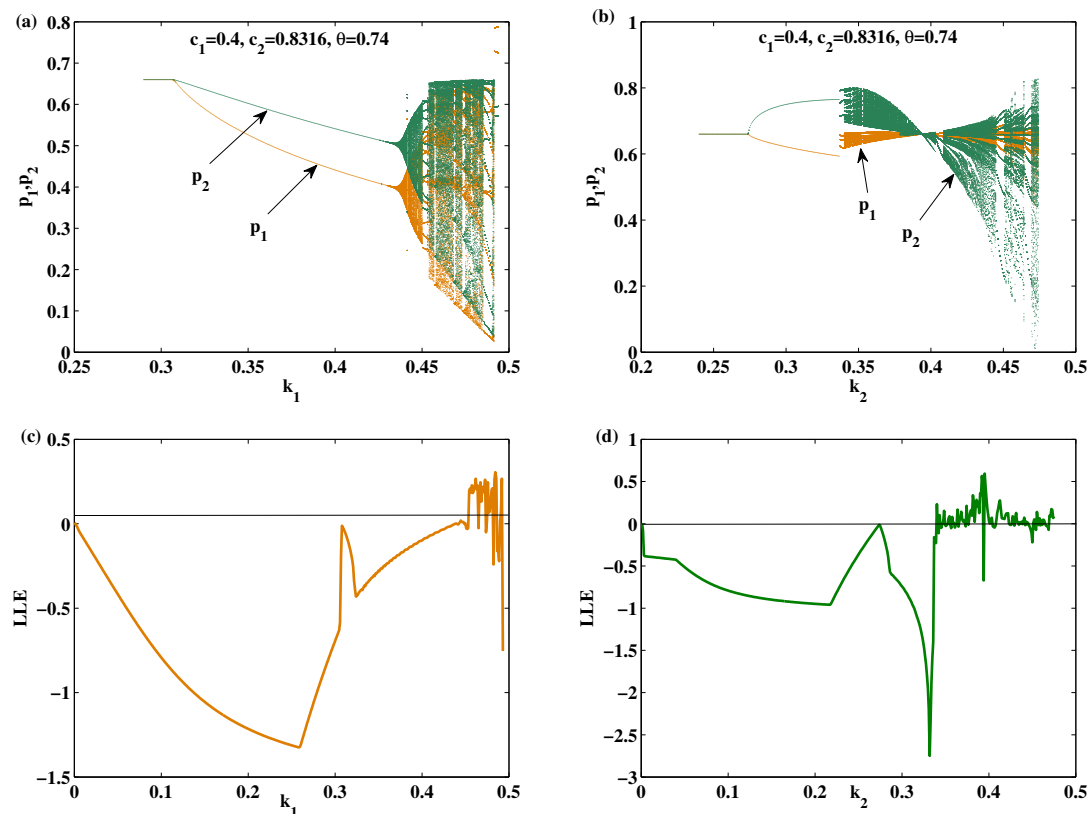


Figure 2. (a) Bifurcation diagrams with respect to p_1 and p_2 on varying k_1 at: $c_1 = 0.4, c_2 = 0.8316, \theta = 0.74$ and $k_2 = 0.1$. (b) Bifurcation diagrams with respect to p_1 and p_2 on varying k_2 at: $c_1 = 0.4, c_2 = 0.8316, \theta = 0.74$ and $k_1 = 0.1$. (c) Largest Lyapunov exponent on varying k_1 for $c_1 = 0.4, c_2 = 0.8316, \theta = 0.74$ and $k_2 = 0.1$ (d) Largest Lyapunov exponent on varying k_2 for $c_1 = 0.4, c_2 = 0.8316, \theta = 0.74$ and $k_1 = 0.1$.

Global Analysis: Multistability and Basin of Attraction

The local analysis discussed previously provides observations about the stability of the map’s equilibrium points around some neighborhoods; it is important to study the global analysis to gain more insight into the complex analysis of the map’s dynamic behavior. Detecting information about the multistability of the map may provide us with some predictions about its future evolution. For that, we perform, in this subsection, a global analysis of the dynamic behavior of the model to obtain projections about the long run of the map’s trajectories. In the previous section, we concluded that the equilibrium point can be destabilized via flip and Neimark–Sacker Bifurcations. Now, we show a variety of different complex dynamic scenarios for the map (13) using numerical simulations. In particular, the chaotic trajectories that can emerge beside the multistability of the map’s behavior where different chaotic attractors may coexist reflect the wide spectrum of the parameter sets. Such complex characteristics are interesting because the demand function adopted by the two firms is linear not nonlinear. Let us start our global analysis by assuming the following parameters set, $c_1 = 0.41, c_2 = 0.45, \theta = 0.9721801, k_1 = 0.006$ and $k_2 = 0.006$. At this set, we have two coincided equilibrium points, $E_{r1} = E_{r2} = (0.4378199, 0.4378199)$ whose Jacobian matrices (14) become,

$$J_{r1} = \begin{bmatrix} 0.81115 & 0.094426 \\ 0.094426 & 0.80574 \end{bmatrix},$$

$$J_{r2} = \begin{bmatrix} 0.81115 & 0.094426 \\ 1 & 0 \end{bmatrix}$$

and the eigenvalues in both regions are $(\lambda_{1r1,2r1}) = (0.90291, 0.71398)$ and $(\lambda_{1r2,2r2}) = (0.91441, -0.10326)$. They are real eigenvalues and lie within the unit circle $|\lambda_{1r1,2r1}| < 1$

and $|\lambda_{1,r2,2r2}| < 1$. In addition, we have $\tau_{r1} = 1.61689$, $\delta_{r1} = 0.64466$, $\tau_{r2} = 0.81115$ and $\delta_{r2} = -0.094426$. It is clear that $|\delta_{r1}| < 1$ and $|\delta_{r2}| < 1$ that means the map (13) is dissipative in both regions of the border curve $\Omega = p_1$ and the triangles of stability are satisfied. Figure 3a shows the basin of attraction of the coincided equilibrium points born on the border curve. It is plotted at the same set of the parameter values. Now, we show the rise of the multistability of attractors, as the speed of the adjustment parameter k_1 increases, the other parameter values remain fixed. We should note that all of the numerical simulations were carried out based on the initial data of decision variables $p_{1,0} = 0.12$ and $p_{2,0} = 0.11$. In the following figures, iterations of the map (13) present different attractors with their basins, using sets of initial conditions at the long run. Increasing the bifurcation parameter k_1 to 0.0659, the equilibrium point becomes unstable and the dynamics of the map converts into a spiral on one side from the border curve, as shown in the top left in Figure 3b. Increasing that parameter further gives rise to larger spiral points and then they convert into a closed invariant curve due to the Neimark–Sacker bifurcation at $k_1 = 0.0664$. This closed invariant curve is tangent to the border curve. This closed invariant curve continues to appear until $k_1 = 0.0796$, where the period-2 cycle is born due to the coexistence of flip bifurcation. It is plotted in Figure 3c with its basin of attraction. As one can see, this period is born on region 1, but its basin is distributed in both regions from the border curve. Increasing k_1 further gives rise to the period-4 cycle, which has a complicated basin of attraction distributed in both regions in Figure 3d. Others increasing in this parameter give four chaotic areas, which start gathering into two chaotic areas, then finally become one chaotic attractor, as shown in Figure 3e,f. It is obvious from the 1D bifurcation diagrams presented in Figure 1c,d that the bifurcation parameter k_1 affects the complex dynamic of the map (13). The dynamics start first with a stable equilibrium point, then closed invariant curves in region 2 appear due to Neimark–Sacker. Afterward, higher periodic cycles and chaotic attractors are born in region 1 due to flip bifurcation. This means that the map's dynamics jumps from Neimark–Sacker to flip bifurcation.

Now, we study another set of parameter values. We assume $c_1 = 0.4$, $c_2 = 0.8316$, $\theta = 0.74$, $k_1 = 0.1$ and $k_2 = 0.1$. At this set, we get two coincided stable equilibrium points born on the border curve $\Omega = p_1$. It is depicted in Figure 4a with its basin of attraction. As previously, we studied the influences of the bifurcation parameter k_1 on the dynamics of the map (13). Increasing k_1 makes the equilibrium point unstable and gives rise to spiral points. Those points are located in region 2, as shown in Figure 4b. They are turned into closed invariant curves in region 2 as k_1 increases further as given in Figure 4c. The closed invariant curves continue to appear because of Neimark–Sacker bifurcation until they turn into a period-11 cycle due to flip bifurcation at $k_1 = 0.451$, and keeping the other parameter values as presented in Figure 4d. It is clear that this period cycle is located in region 2 and it does not cross the border curve that means the dynamic of the map (13) is only obtained by the part defined in this region. In Figure 4e, we obtain a period-11 cycle located in region 2 with a chaotic attractor that crosses the border curve and is distributed in both regions at $k_1 = 0.452$. It is also clear that the phase plane becomes quite complicated. Increasing k_1 to 0.46 gives a chaotic attractor of the map in both regions and passes through the border curve. This chaotic attractor continues to appear until a period-9 cycle is born at $k_1 = 0.4736$ with the other parameter values fixed. Figure 5a displays this cycle with its complicated basin of attraction, and it is clear it has points jumping from region 1 to region 2. This indicates that the map (13) must be manipulated and studied as a piecewise smooth map. When k_1 increases further, a one-piece chaotic attractor continues to appear and pass through the border curve. After that, further increasing in the parameter k_1 gives birth to an additional period-10 cycle crossing the border curve. Figure 5b displays this period cycle with its basin of attraction. As k_1 increases, further higher period cycles that are followed by chaotic attractors passing through the border curve arise. After that, the dynamic of the map changes to a period-2 cycle at $k_1 = 0.5$, which is followed by a period-4 cycle at $k_1 = 0.501$ and both cycles are located in region 1. We end our discussion here by presenting the influences of the parameter θ when fixing the map's parameters. It is

obvious that both equilibrium points depend on that parameter, which means we will get two different equilibrium points. In that case, the dynamic of the map will be related to only one region and we will have only one equilibrium point; the other point will be called the virtual equilibrium point. We present, in Figure 5c,d, the bifurcation diagrams when varying the parameter θ . Influences of that parameter on the map's dynamic are left to the readers.

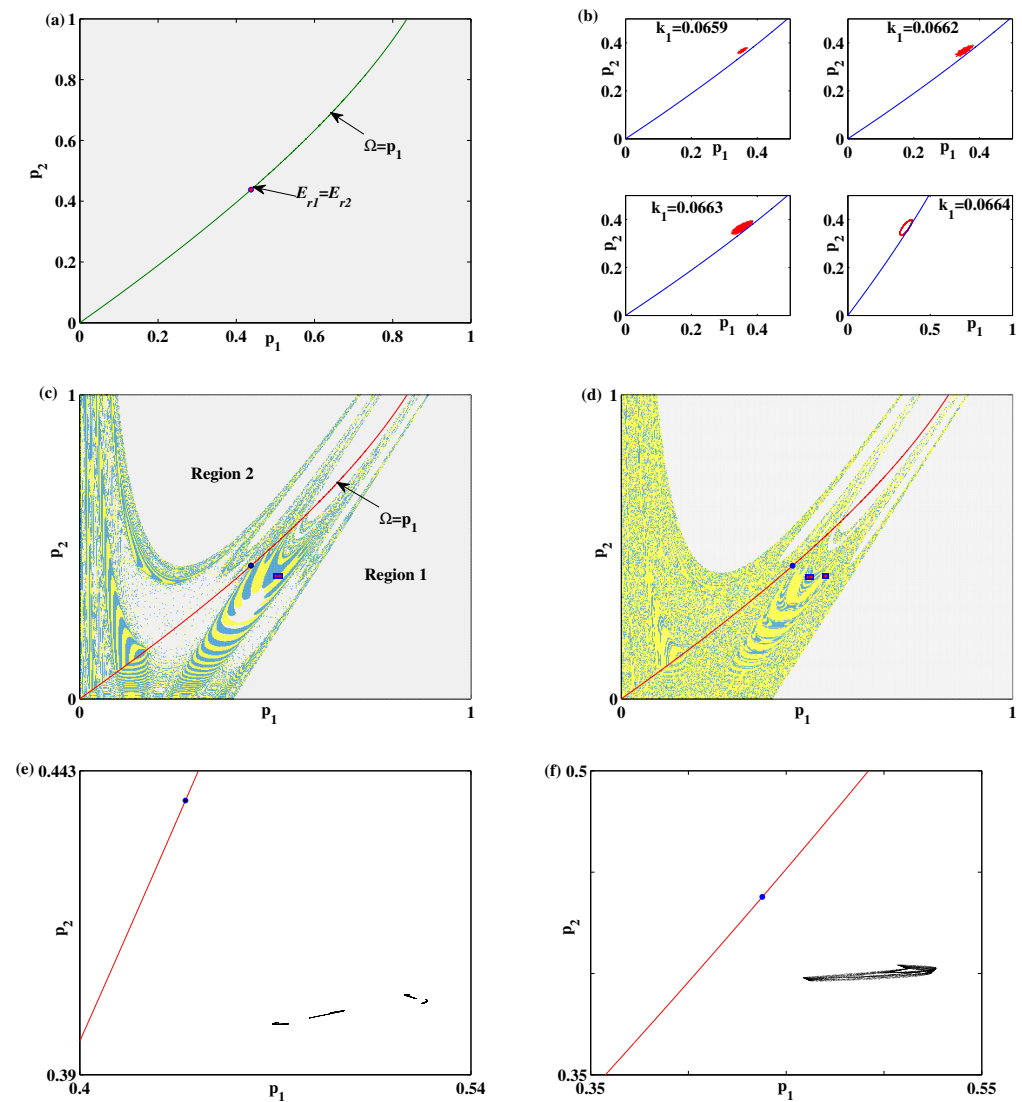


Figure 3. (a) The basin of attraction of the equilibrium points. (b) Spiral and closed invariant curves at different values of k_1 . (c) Basin of attraction of period-2 cycle at $k_1 = 0.0827$. (d) Basin of attraction of period-4 cycle at $k_1 = 0.0834$. (e) Phase plane for the four pieces chaotic areas at $k_1 = 0.0836$. (f) Phase plane for the one piece chaotic attractor at $k_1 = 0.0845$. Other parameters values are: $c_1 = 0.41, c_2 = 0.45, \theta = 0.9721801$ and $k_2 = 0.006$.

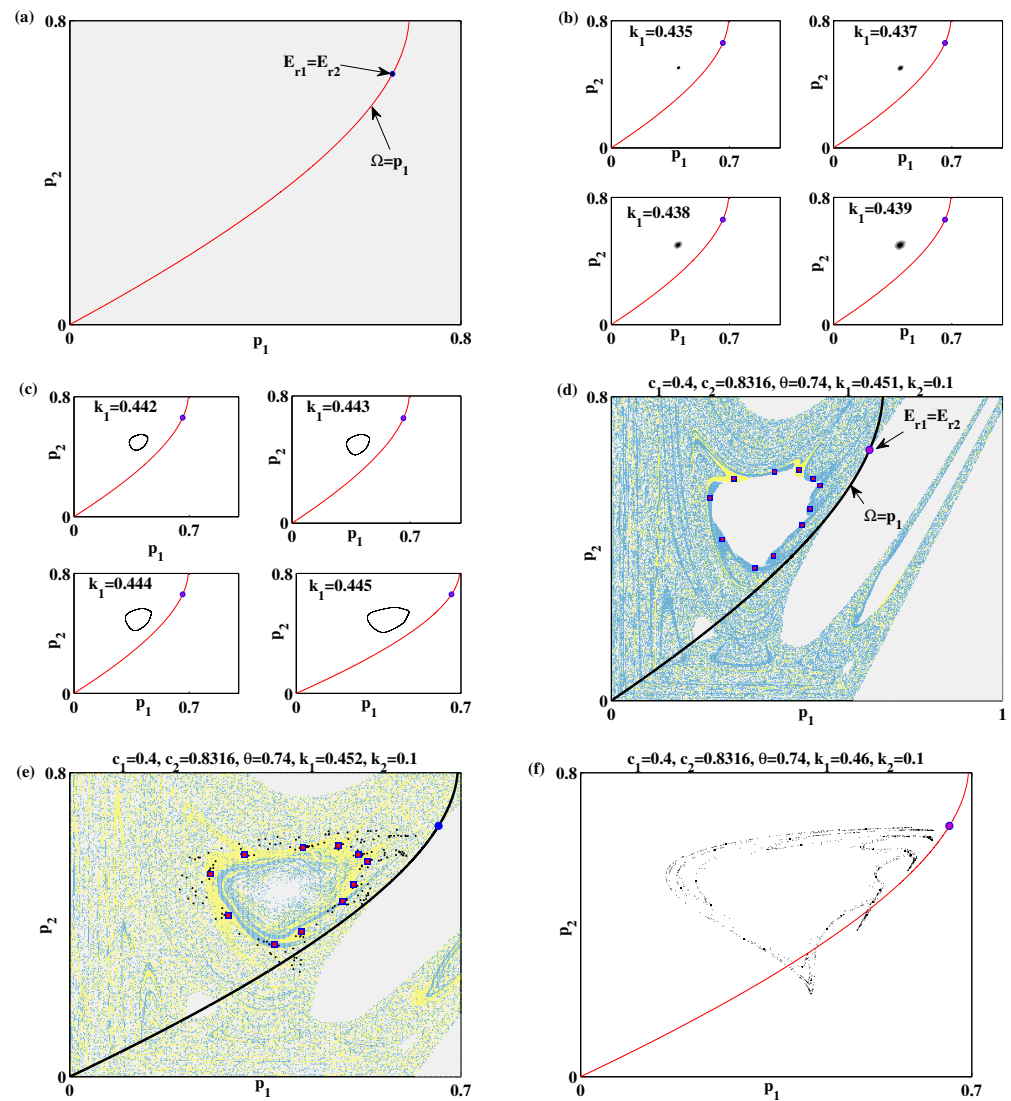


Figure 4. (a) The stable equilibrium point with its basin of attraction around it. Parameters values are $c_1 = 0.4, c_2 = 0.8316, \theta = 0.74, k_1 = 0.1$ and $k_2 = 0.1$. (b) Spiral points at different values of k_1 . (c) Closed invariant curves at different values of k_1 . (d) The basin of attraction for the period-11 cycle at $k_1 = 0.451$. The gray color denotes divergent and infeasible trajectories. (e) Basin of attraction of the period-11 cycle with the chaotic attractor. (f) Phase plane of the chaotic attractor.

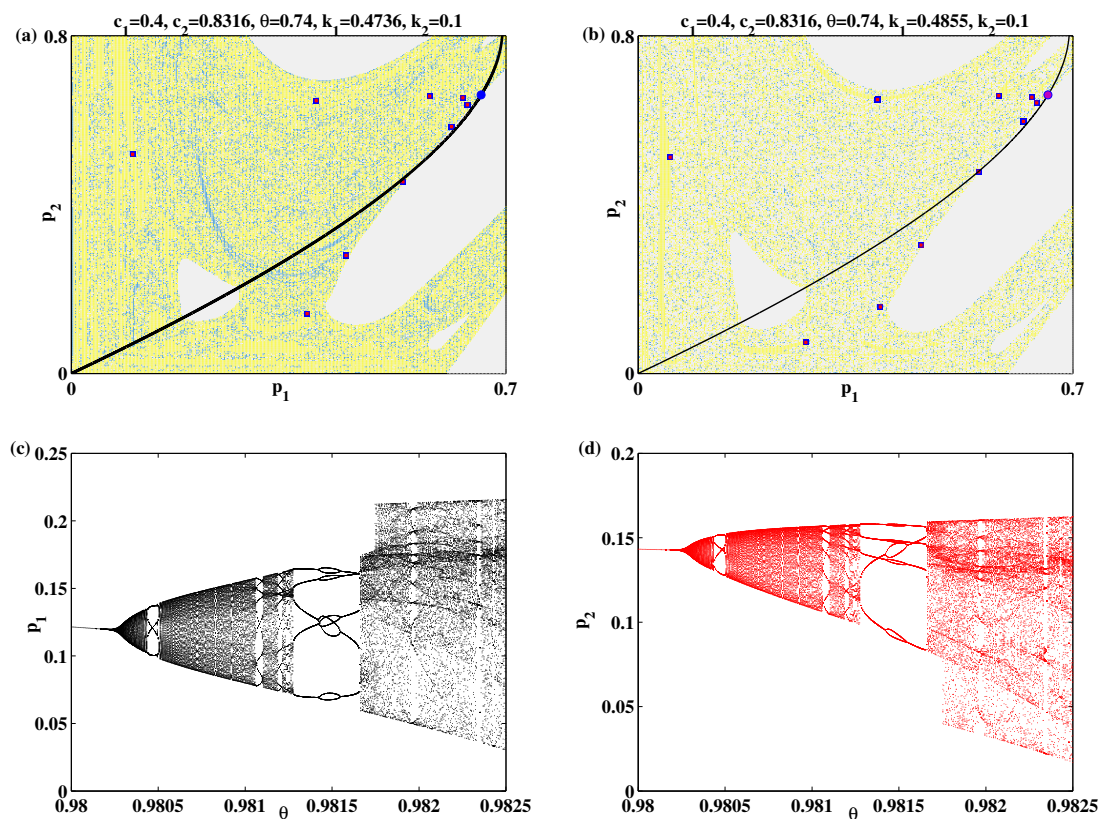


Figure 5. (a) The basin of attraction for the period-9 cycle. (b) The basin of attraction for the period-10 cycle. (c) Bifurcation diagram with respect to p_1 on varying θ at: $c_1 = 0.2, c_2 = 0.1, k_1 = 0.1$ and $k_2 = 0.1$. (d) Bifurcation diagram with respect to p_2 on varying θ at: $c_1 = 0.2, c_2 = 0.1, k_1 = 0.1$ and $k_2 = 0.1$.

5. Conclusions

In this paper, we introduced and investigated a piecewise smooth Bertrand game. Our results—by the global analysis—showed multiple attractors due to border collision bifurcations. This is because the map's phase plane was divided into two regions by a border curve, which has a crucial role in the global dynamics. We analyzed the behavior of the equilibrium points and their stabilities. For two coincided equilibrium points born on the border curve, we showed that they become unstable due to two types of bifurcations, which occurred simultaneously. First, the equilibrium points became unstable due to the coexistence of closed invariant curves by Neimark–Sacker, then those closed invariant curves were destroyed, and different periodic cycles and chaotic attractors emerged because of flip bifurcation. This situation was shown by a 1D bifurcation analysis and then globally by presenting other complex dynamic characteristics, which occurred in each region where the map was defined.

Funding: This research was funded by King Saud University.

Institutional Review Board Statement: Not applicable.

Informed Consent Statement: Not applicable.

Data Availability Statement: Not applicable.

Acknowledgments: Research supporting project number (RSP-2021/167), King Saud University, Riyadh, Saudi Arabia.

Conflicts of Interest: The author declares that there are no conflicts of interest.

References

1. Cournot, A. *Récherches sur les Principes Mathématiques de la Théorie des Richesses*, Dunod, Paris, 1838. Available online: <https://www.jstor.org/stable/27579580> (accessed on 5 September 2021).
2. Bertrand, J. *Theorie Mathématique de la Richesse Sociale*. *J. Savants* **1883**, *48*, 499–508.
3. Askar, S.S. On complex dynamics of cournot-bertrand game with asymmetric market information. *Appl. Math. Comput.* **2021**, *393*, 125823.
4. Askar, S.S. Duopolistic Stackelberg game: Investigation of complex dynamics and chaos control. *Oper. Res.* **2018**, *20*, 1685–1699. [[CrossRef](#)]
5. Askar, S.S.; Abouhawwash, M. Quantity and price competition in a differentiated triopoly: Static and dynamic investigations. *Nonlinear Dyn.* **2018**, *91*, 1963–1975 [[CrossRef](#)]
6. Askar, S.S.; Elettrey, M.F. The impact of cost uncertainty on Cournot oligopoly games. *Appl. Math. Comput.* **2017**, *312*, 169–176. [[CrossRef](#)]
7. Askar, S.S. Triopoly Stackelberg game model: One leader versus two followers. *Appl. Math. Comput.* **2018**, *328*, 301–311. [[CrossRef](#)]
8. Li, Y.; Wang, L. Chaos in a duopoly model of technological innovation with bounded rationality based on constant conjectural variation. *Chaos Solitons Fractals* **2019**, *120*, 116–126. [[CrossRef](#)]
9. Elsadany, A.A.; Awad, A.M. Dynamics and chaos control of a duopolistic Bertrand competitions under environmental taxes. *Ann. Oper. Res.* **2018**, *274*, 211–240. [[CrossRef](#)]
10. Agiza, H.N.; Elsadany, A.A. Nonlinear dynamics in the Cournot duopoly game with heterogeneous players. *Phys. A* **2003**, *320*, 512–524. [[CrossRef](#)]
11. Askar, S.S.; Alshamrani, A.M.; Alnowibet, K. Dynamic Cournot duopoly games with nonlinear demand function. *Appl. Math. Comput.* **2015**, *259*, 427–437. [[CrossRef](#)]
12. Hommes, C. *Behavioral Rationality and Heterogeneous Expectations in Complex Economic Systems*; Cambridge University Press: Cambridge, UK, 2013.
13. Peng, Y.; Lu, Q.; Xiao, Y.; Wu, X. Complex dynamics analysis for a remanufacturing duopoly model with nonlinear cost. *Phys. A* **2019**, *514*, 658–670. [[CrossRef](#)]
14. Elsadany, A.A.; Awad, A.M. Dynamical analysis and chaos control in a heterogeneous Kopel duopoly game. *Indian J. Pure Appl. Math.* **2016**, *47*, 617–639. [[CrossRef](#)]
15. Askar, S.S.; Alshamrani, A.M.; Alnowibet, K. The arising of cooperation in Cournot duopoly games. *Appl. Math. Comput.* **2016**, *273*, 535–542. [[CrossRef](#)]
16. Shi, L.; Sheng, Z.H.; Xu, F. The dynamics of competition in remanufacturing: A stability analysis. *Econ. Model.* **2015**, *50*, 245–253. [[CrossRef](#)]
17. Gardini, L.; Sushko, I.; Matsuyama, K. 2D discontinuous piecewise linear map: Emergence of fashion cycles. *Chaos* **2018**, *28*, 055917. [[CrossRef](#)]
18. Commendator, P.; Kubin, I.; Petraglia, C.; Sushko, I. Regional integration, international liberalisation and the dynamics of industrial agglomeration. *J. Econ. Dyn. Control.* **2014**, *48*, 265–287. [[CrossRef](#)]
19. Commendator, P.; Kubin, I.; Mossay, P.; Sushko, I. The role of centrality and market size in a four-region asymmetric new economic geography model. *J. Evol. Econ.* **2017**, *27*, 1095–1131. [[CrossRef](#)]
20. Radi, D.; Gardini, L.; Avrutin, V. The role of constraints in a segregation model: The symmetric case. *Chaos Solitons Fractals* **2014**, *66*, 103–119. [[CrossRef](#)]
21. Radi, D.; Gardini, L.; Avrutin, V. The role of constraints in a segregation model: The asymmetric case. *Discret. Dyn. Nat. Soc.* **2014**, *2014*, 569296. [[CrossRef](#)]
22. Agliari, A.; Gardini, L.; Puu, T. Global bifurcations in duopoly when the Cournot point is destabilized via a subcritical Neimark bifurcation. *Int. Game Theory Rev.* **2006**, *8*, 1–20. [[CrossRef](#)]
23. Puu, T. A new approach to modeling Bertrand duopoly. *Rev. Behav. Econ.* **2017**, *4*, 51–67. [[CrossRef](#)]
24. Singh, N.; Vives, X. Price and quantity competition in a differentiated duopoly. *Rand J. Econ.* **1984**, *15*, 546–554. [[CrossRef](#)]
25. Askar, S.S. The rise of complex phenomena in Cournot duopoly games due to demand functions without inflection points. *Commun. Nonlinear Sci. Numer. Simul.* **2014**, *19*, 1918–1925. [[CrossRef](#)]
26. Askar, S.S.; Al-Khedhairi, A. Analysis of nonlinear duopoly games with product differentiation: Stability, global dynamics, and control. *Discret. Dyn. Nat. Soc.* **2017**, *2017*, 2585708. [[CrossRef](#)]
27. Agiza, H.N.; Elsadany, A.A. Chaotic dynamics in nonlinear duopoly game with heterogeneous players. *Appl. Math. Comput.* **2004**, *149*, 843–860. [[CrossRef](#)]